Molecular Modeling Study to the Relation between Structure of LPEI, Including Water-Induced Phase Transitions and CO_2 Capturing Reactions

Buijs, W.

DOI
10.1021/acs.iecr.1c00846

Publication date
2021

Document Version
Final published version

Published in
Industrial and Engineering Chemistry Research

Citation (APA)
Buijs, W. (2021). Molecular Modeling Study to the Relation between Structure of LPEI, Including Water-Induced Phase Transitions and CO_2 Capturing Reactions. *Industrial and Engineering Chemistry Research*, *60*(30), 11309-11316. https://doi.org/10.1021/acs.iecr.1c00846

I&EC research
Industrial & Engineering Chemistry Research
pubs.acs.org/IECR
Article

Molecular Modeling Study to the Relation between Structure of LPEI, Including Water-Induced Phase Transitions and CO_2 Capturing Reactions

W. Buijs*

Cite This: *Ind. Eng. Chem. Res.* 2021, 60, 11309−11316

ABSTRACT: A molecular modeling study was carried out on linear polyethyleneimine (LPEI) to determine the CO_2 capturing process taking into account structural changes of the material at various amounts of H_2O. Until now, CO_2 capture by LPEI was described as a combination of carbamic and carbonic acid formation. It was found that humidification below the melting point of LPEI leads to the formation of an LPEI/0.5H_2O type of phase. Such a type of phase leads to CO_2 capture exclusively via carbonic acid formation, stabilized by secondary amines via ammonium bicarbonate and H-bridged amine carbonic acid complexes. Both the strong physisorption CO_2 complex and the low activation barrier for carbonic acid formation contribute to the overall process. Only in the absence of H_2O, carbamic acid formation is possible. Thus, under CO_2 capturing process conditions, carbonic acid formation seems to be the only option as H_2O will be present in flue gas.

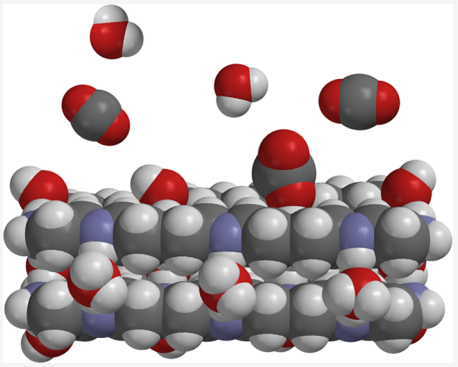

INTRODUCTION

At present, the world is facing the effects of climate change due to anthropogenic CO_2 emissions.[1] These CO_2 emissions can be divided into large and small point emission sources with an approximately equal contribution.[2] CO_2 capture and final geological sequestration is required to lower the atmospheric CO_2 level and mitigate the adverse effects of climate change actively. Many materials have been proposed for CO_2 capture, including polyamine resins like polyethyleneimine (PEI) and Lewatit R VP OC 1065.[3−8] They have shown excellent behavior with respect to the CO_2 process cycle capacity, and solutions have been put forward to avoid several deactivation processes like oxidative degradation, formation of urea, and deactivation by SO_2.[9−12] The CO_2 capturing process is usually described as a combination of the formation of carbamic acid and carbonic acid from the amines and CO_2 in close analogy to CO_2 capture with amines in an aqueous environment. In 2012, Lee and Kitchin[13] developed molecular descriptors derived from a range of functional groups to describe the above-mentioned reactions between amines and CO_2. Very recently, a joint experimental and computational study has tried to develop a unified approach to CO_2−amine reaction mechanisms.[14] It was found that an additional amine or H_2O is required (by acting as a catalyst) to enable the reaction to form a carbamic acid or carbonic acid and that carbonic acid formation is usually not the result of hydrolysis of carbamic acid. However, as such general approaches are useful, they do not consider the decisive role of the three-dimensional (3D) structure of the CO_2 absorbing material for CO_2 physisorption and the required catalysis to yield a carbamic or carbonic acid.

It was already shown in a previous molecular modeling study[15] that direct air capture of CO_2 on Lewatit R VP OC 1065 proceeds exclusively via the formation of carbamic acid and that the actual operating catalytic species are causally related to the 3D structure of the Lewatit R VP OC 1065 resin both in the absence and presence of H_2O. Until now, no such study was published on linear polyethyleneImine (LPEI). This molecular modeling study tries to identify the CO_2 capturing process of LPEI starting from known experimental data on its structure as a function of the amount of water.

MOLECULAR MODELING

All molecular simulations were performed using Wavefunction's Spartan'18 suite.[16] Molecular mechanics (MMFF) was used to study basic structural features of LPEI, with and without H_2O or CO_2 physisorption. The results of that study were used to select candidates for chemisorption by reactions between the amine, H_2O, and CO_2, using quantum chemical calculations. All structures were fully optimized using density functional theory with (DFT) B3LYP/6-31*G. Transition states were identified and characterized using their unique imaginary vibrational frequency. In addition, the conductor-

Received: March 2, 2021
Revised: July 5, 2021
Accepted: July 12, 2021
Published: July 22, 2021

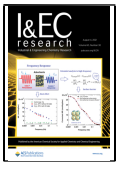

https://doi.org/10.1021/acs.iecr.1c00846
Ind. Eng. Chem. Res. 2021, 60, 11309−11316

like polarizable continuum model (C-PCM)[35] was used in combination with B3LYP/6-31G* to account for LPEI as a medium. Physisorption, reaction, and activation enthalpies were calculated based upon total energies and enthalpy corrections. In some physisorption cases, experimentally known entropy corrections were used to allow an estimate of ΔG values. All molecular (ensemble) structures are available in the Supporting Information.

RESULTS AND DISCUSSION

PEI is a very versatile polymer with a long history and many applications. Among the applications are typical industrial ones like corrosion inhibitor,[17−19] electrical energy storage device, personal care as a cosmetic ingredient, and several biological applications.[20−23] PEI is being used in many forms and different average molecular weights. PEI can be divided into 3 forms: linear, branched, and dendrimeric PEI. This study will focus on linear PEI (LPEI). One of the advantages of a polymer with such a long history is that the structure of LPEI is known since 1981. In a series of articles,[24−26] Chatani et al. describe the various crystal structures of LPEI as a function of the amount of H_2O incorporated in the crystalline phase:

1. Anhydrous LPEI has a double-stranded helix structure below its melting point at 60 °C; above the melting point, the double-stranded helix structure transforms into all-trans linear chains.
2. LPEI/0.5 H_2O built up from all-trans linear chains of LPEI held together by H-bridging H_2O molecules in a ratio of O/N = 0.5 ⇔ H_2O content: 17 wt %.
3. LPEI/1.5 H_2O built up from all-trans linear chains of LPEI held together by H-bridging H_2O molecules in a ratio of O/N = 1.5 ⇔ H_2O content: 38 wt %.
4. LPEI/2.0 H_2O built up from all-trans linear chains of LPEI held together by H-bridging H_2O molecules in a ratio of O/N = 2.0 ⇔ H_2O content: 45 wt %.

Details of the elucidation of these structures can be found in the original articles cited and in various other later publications[27−29] wherein the phase transitions of these crystal structures as a function of [H_2O] and temperature were studied in detail. In 2015 and 2017, two important studies[30,31] were published wherein the CO_2 uptake of LPEIs with average molecular weights varying from 2500 to 25 000 was experimentally determined quantitatively under dry and humid conditions. As these studies contain valuable quantitative data on adsorption and desorption of CO_2 over a wide range of CO_2 levels and temperatures, they were used to calibrate the molecular modeling results.

The molecular modeling study starts from the double-stranded helix structure of anhydrous LPEI, then pays attention to the melting process into linear chains, and finally, assesses the structure of LPEI/0.5H_2O, with respect to their role in the CO_2 capturing process. Unfortunately, these crystal structures are not available in the Cambridge Structural Database (CSD).[32] Fortunately, Herlem et al. published a quantum chemical DFT study of the electronic and structural properties of the crystalline anhydrous LPEI[33] in 2004 and they kindly provided the double-stranded helix structure of LPEI. Figures 1 and 2 are typical examples.

The front view shows the double-stranded helices tightly packed in a hexagonal array. The primary amines seem to be the only accessible groups for H_2O or CO_2. Figure 2 shows a side view of a single double-stranded helix displayed in space

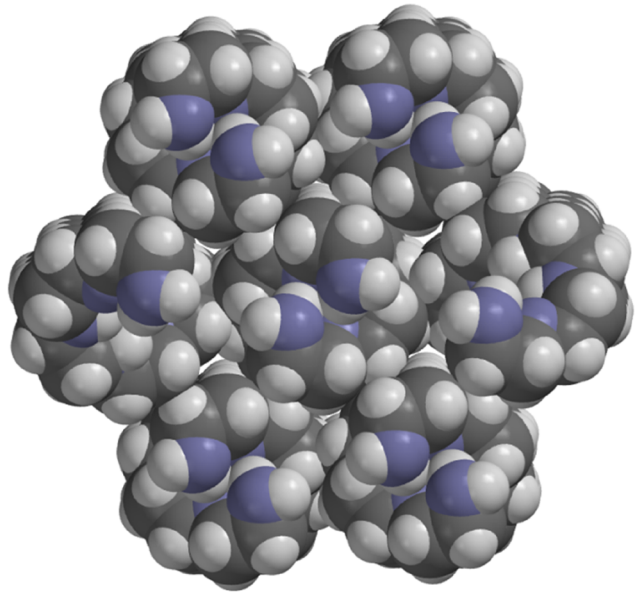

Figure 1. Front view of the double-stranded helix structure of LPEI;[33] display model: space filling with C: gray, N: blue, and H: white.

filling and ball & spoke mode. The space filling view shows that all secondary amine groups even in a single double-stranded helix are completely shielded by the $-CH_2CH_2$ groups and are not accessible to either H_2O or CO_2. The ball & spoke view shows that H-bridges between the amine groups of the two strains are not between the parallel amine groups but between an amine of one strand and the next secondary amine of the second strand with an NH−N distance of 2.347 Å, significantly longer than the NH−N distance in $CH_3NH_2-NH_2CH_3$ of 2.192 Å. Furthermore, not all amine groups are involved in H-bridges between the two strands: every third amine group does not form an H-bridge with an amine group of the second strand but has interactions with two β-amine groups of the same strand with an NH−N distance of 2.583 Å. The N−N distances between the primary amines are 3.464 and 3.471 Å.

Figure 3 shows two LPEI hexamers as a model of the melting process of one double-stranded helix into a pair of LPEI chains at 60 °C and probably too from the amorphous regions in the crystalline polymer. From the study of Hashida et al.,[29] for an LPEI with a melting point of 60 °C, it is clear that single chains of LPEI are observed only at temperatures above 66 °C. An MMFF conformer distribution calculation yielded the linear all-trans conformer as the best by 9.81 kJ/mol compared to the second conformer. At first glance in space filling display, the LPEI hexamers look like trimers because only four amine groups are visible but the remaining three amine groups are on the backside in the trans position as can be seen from the ball & spoke display. The NH−N distances in the LPEI pair vary from 2.367 Å for the two primary amine H-bridges to 2.871 Å for the secondary amines. The latter are no longer recognized as H-bridges by the program and significantly larger than in the double-stranded helix. The N−N distance between the primary amines is between 3.298 and 3.346 Å and the N−N distances between the secondary amines range from 3.739 to 3.836 Å.

The differences in N−N distances are caused by variations in the trans $NH(CH_2)_2NH$ positions, which are recognized by the program but usually do not have a practical meaning as N-inversion is fast. Unlike in the double-stranded helix structure,

https://doi.org/10.1021/acs.iecr.1c00846
Ind. Eng. Chem. Res. 2021, 60, 11309−11316

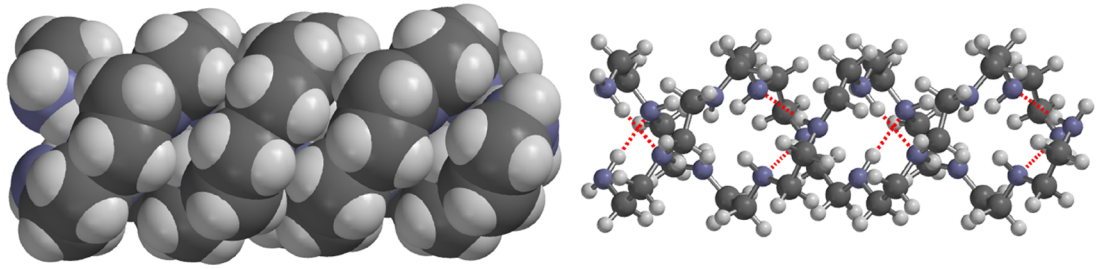

Figure 2. Side view of $(LPEI\text{-}9)_2$ as one double-stranded helix;[33] display model: space filling and ball & spoke with C: gray, N: blue, and H: white. H-bridges: red dotted lines.

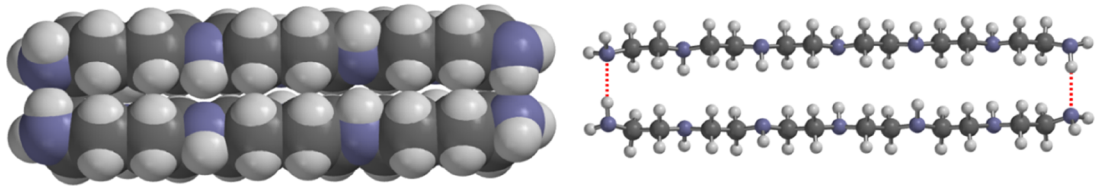

Figure 3. Side view of a pair of all-trans LPEI hexamers; B3LYP/6-31G*; display model: space filling and ball & spoke with C: gray, N: blue, and H: white. H-bridges: red dotted lines.

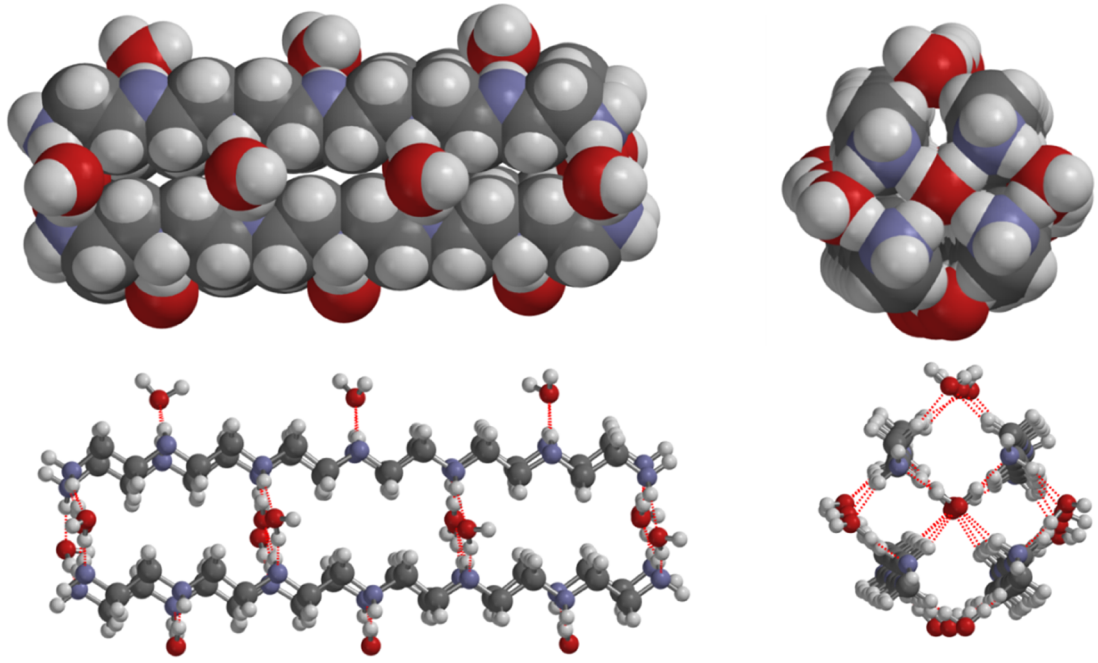

Figure 4. Side and front views of the cluster $(LPEI\text{-}6)_4(H_2O)_{18}$ as a model for the crystal structure of LPEI/0.5 H_2O; B3LYP/6-31G*; display model: space filling and ball & spoke with C: gray, N: blue, and H: white. H-bridges: red dotted lines.

in the all-trans LPEI pair secondary amines are no longer shielded and are accessible for H_2O or CO_2. Hexamers were chosen as it turned out that on B3LYP/6-31G* geometry optimization the double-stranded helix structure remains intact only from chain length n = 6. The B3LYP/6-31G* interaction enthalpies of the two hexamers in the double-stranded helix and in the all-trans conformation are −60.5 and −57.5 kJ/mol, respectively, resulting in an energy difference of 3 kJ/mol only in favor of the double-stranded helix structure. Furthermore, the interaction enthalpy between two pairs of linear all-trans hexamers is −27.5 kJ/mol. With some care, it can be concluded that melting of the double-stranded helix structure of LPEI at 60 °C will yield pairs of all-trans LPEI chains, which in turn at higher temperatures will be converted to single chains.

LPEI/0.5H_2O. The addition of H_2O to anhydrous LPEI at temperatures below its melting range almost exclusively leads to LPEI/0.5 H_2O and depending on process conditions (temperature, amount of water) thereafter to LPEI/1.5 H_2O and LPEI/2.0 H_2O.[29] Figure 4 shows a cluster model $(LPEI\text{-}6)_4(H_2O)_{18}$ of the crystal structure of LPEI/0.5H_2O. The cluster was built from four all-trans PEI hexamers wherein each amine group is coordinated to two H_2O molecules. Four H_2O molecules inside the four chains are coordinated to four amine groups and 14 H_2O molecules on the outsides to two amine groups. The coordination around the oxygen of the four H_2O molecules between the four chains is close to square planar.

https://doi.org/10.1021/acs.iecr.1c00846
Ind. Eng. Chem. Res. 2021, 60, 11309−11316

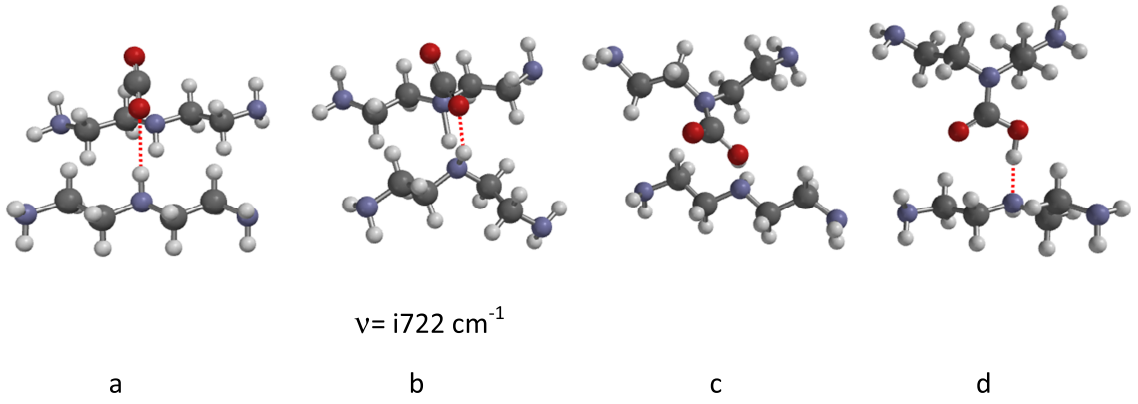

Figure 5. LPEI dimer pair: (a) $(LPEI\text{-}2)_2(CO_2)$, (b) transition state $(LPEI\text{-}2)_2(CO_2)$, (c) $(LPEI\text{-}2)_2(NHCO_2H\text{-anti})$, and (d) $(LPEI\text{-}2)_2(NHCO_2H)$; B3LYP/6-31G*; display model: ball & spoke with C: gray, N: blue, and H: white. H-bridges: red dotted lines.

The angle N−HOH−N = 100.8° and the angle NH−O−HN = 90.0°. The distances OH−N and NH−O are 1.932 and 2.205 Å respectively, which are close to the corresponding values obtained with a CH_3NH_2-H_2O system. As the secondary amine groups are trans-oriented, the coordinating H_2O molecules appear in an alternating mode above and below, and in front and to the back of each pair of oligomeric chains. The amines and the coordinated H_2O molecules build alternating planes perpendicular to the oligomeric chains. All computational values are in line with the crystal structure described by Hashida et al.;[29] however, they reported relatively large standard deviations in distances and angles. The three H_2O molecules on top of the cluster have partly adopted a more tetrahedral coordination in the absence of additional coordinating amine groups, which seems realistic at the edge of a crystal-like cluster.

The overall B3LYP/6-31G* interaction enthalpy of $(LPEI\text{-}6)_4(H_2O)_{18}$ calculated from $(LPEI\text{-}6)_4$ and 18 H_2O yielded −1222.0 kJ/mol corresponding to −67.9 kJ/mol added H_2O molecule. The average interaction enthalpy of −67.9 kJ/mol is large enough to compensate the entropy contribution[34] of 36.3 kJ/mol at 60 °C, yielding a ΔG of −31.6 kJ/mol. The uptake of H_2O is clearly an exothermic process. To get an impression of the B3LYP/6-31G* interaction enthalpy between the four chains and the 4 H_2O molecules showing almost square planar coordination, the B3LYP/6-31G* interaction enthalpy between the corresponding $(LPEI\text{-}6)_4(H_2O)_4$ cluster with $(LPEI\text{-}6)_4$ and 4 H_2O yielded −342.0 or −85.5 kJ/mol added H_2O molecule, significantly lower than the average value of −67.9 kJ/mol. It is quite logical that the H_2O molecules above, below, in front, and to the back side of the cluster are more loosely bound than the four H_2O molecules inside and this offers an opportunity to coordinate additional H_2O or CO_2 molecules. LPEI/1.5 H_2O and LPEI/2.0 H_2O are built up from all-trans linear LPEI chains like LPEI/0.5 H_2O. The additional water molecules form H-bridged networks of five- and six-membered rings with each other between the linear chains and with the secondary amines in the chains. It is very unlikely that they will be formed under CO_2 capturing process conditions. Zhang et al.[31] reported a maximum H_2O uptake of a 12 mmol H_2O/g sorbent at 25 °C, which is very close to a H_2O/amine ratio in LPEI/0.5 H_2O.

CO_2 Capturing Reactions. *Dry Conditions.* Zhang et al.[30] reported a CO_2 uptake of FS-LPEI (LPEI: M_w = 5000 g/mol) under dry conditions ranging from ∼1 mmol/g of the sorbent at 25 °C to ∼3.5 mmol/g of the sorbent at 70 °C. At higher temperatures, competing CO_2 desorption already lowers the CO_2 uptake. Below the melting point of LPEI(5000) 54−59 °C, CO_2 adsorption is similar for all CO_2 concentrations, ranging from 5 to 95%. LPEI(5000) contains >98% of secondary amines, and under dry conditions, carbamic acid or carbamate are the only species that can be formed. From the discussion above, it is clear that the crystalline part of LPEI, consisting of double-stranded helix regions, is not involved in the CO_2 capturing reactions because the secondary amines are completely shielded. Thus, the amorphous part, at least partly consisting of pairs of LPEI chains wherein the secondary amines are not shielded, remains. As a model system, a pair of all-trans LPEI dimers was chosen because this system still contains the essential structural features discussed above. The absolute error in DFT calculations is dependent on the size; thus, the smallest possible system will minimize that error albeit that the final accuracy is also largely determined by cancelation of errors in the calculation of energy differences between similar systems. However, the medium effect of the LPEI polymer itself could be missed. An attempt to account for the medium effect is to apply the C-PCM solvation model on these small systems. Figure 5 shows the formation of carbamic acid from a pair of secondary amines and CO_2.

The CO_2-physisorption complex (a) has a ΔH of −15.7 kJ/mol. The forward and backward activation barriers are 80.6 and 76.8 kJ/mol respectively, indicative of a fast equilibrium process. The animation of the imaginary vibration of the transition state (b) shows the simultaneous formation of the N−C (CO_2) bond, proton transfer from the first secondary amine to the second, and proton transfer from the second secondary amine to the oxygen of CO_2. The initial product, the carbamic acid in its anticonfiguration (c), and the final product, the carbamic acid (d), show H-bridges to the opposite secondary amine.

Several studies[36−40] have presented experimental and computational evidence (IR, NMR) for the formation of ammonium carbamate and bicarbonate species under various circumstances and materials. The computational work largely depends on the applied methods and actual structures. Applying B3LYP and MO6-2X functionals on the LPEI dimers with basis sets ranging from 6-31G* until 6-311+G** yielded amine carbamic acid complexes only, even on starting from the corresponding ammonium carbamate structures. However, applying the C-PCM solvation model yielded both an amine carbamic acid and an ammonium carbamate complex as (meta)stable species already on applying a nonpolar solvent (ε

https://doi.org/10.1021/acs.iecr.1c00846
Ind. Eng. Chem. Res. 2021, 60, 11309−11316

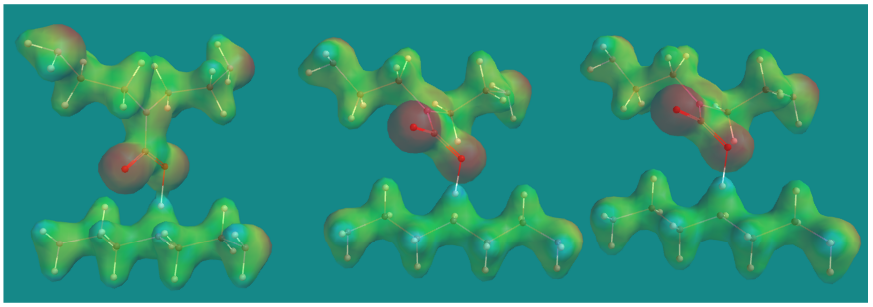

Figure 6. $(LPEI\text{-}2)_2(NHCO_2^-\text{-}H_2NR_2^+)$ complexes after B3LYP/6-31G* optimization applying the C-PCM model; display model: ball & wire. Surface: electrostatic potential mapped on 0.08 e/au^3.

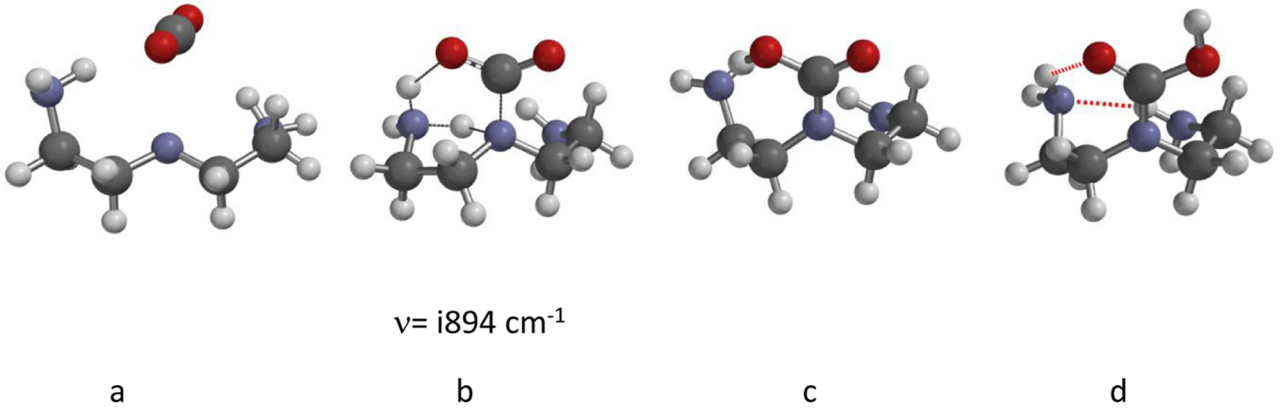

Figure 7. Single-chain LPEI dimer cluster: (a) $(LPEI\text{-}2)(CO_2)$, (b) transition state $(LPEI\text{-}2)(CO_2)$, (c) $(LPEI\text{-}2)(NHCO_2H\text{-anti})$, and (d) $(LPEI\text{-}2)(NHCO_2H)$; B3LYP/6-31G*; display model: ball & spoke with C: gray, N: blue, and H: white. H-bridges: red dotted lines.

= 7.43). Increasing ε from 7.43 via 37.2 (to mimic a polar solvent) to 78.3 (to mimic aqueous solvation) lowered the energy difference between the amine carbamic acid and the ammonium carbamate complex from 42.9 to 20.5 kJ/mol still largely in favor of the amine carbamic acid complex. Figure 6 shows the three ammonium carbamate structures obtained with the C-PCM model representing various solvents. The CO−H and H−NHR_2 distances are 1.466 and 1.123, 1.545 and 1.087, and 1.545 and 1.087 Å for ε = 7.43, 37.2, and 78.3, respectively. In the nonpolar solvent situation, the proton transfer from the carbamic acid to the secondary amine is not complete, as can be seen from the isosurface plot: there is remaining electron density between the oxygen and the hydrogen. The other two situations yield essentially identical geometries, indicating that the proton transfer from the carbamic acid to the secondary amine is complete from ε = 37.2. The dielectric constant for PEI is reported to be between 3 and 4,[41] and thus, the nonpolar solvent situation seems to be the most applicable one. Summarizing, it can be said that neither the use of a different functional nor the application of the C-PCM solvation model points toward a significant presence of the ammonium carbamate.

Formation of the carbamic acid leads locally to a considerable widening of the distance between the pair of LPEI chains. As a result, the overall reaction enthalpy of −54.2 kJ/mol is rather low compared with a ΔH-value of −71.7 kJ/mol for a carbamic acid H-bridged to a secondary amine not being a part of an LPEI chain. The difference between these values is caused by the loss of interaction of the two LPEI chains as a result of carbamic acid formation and hindered H-bridging with a secondary amine. The ΔH of −54.2 kJ/mol agrees well with the reported[30] value for ΔH of −53 kJ/mol of LPEI(5000) and LPEI(10 000) at 55 °C. The temperature of 55 °C is important because in that area the polymer starts to melt, leading to the formation of pairs of LPEI chains required for this reaction mechanism. At even higher temperatures, the melting process will eventually lead to the formation of single chains.[29] Therefore, a CO_2 capturing process starting from single LPEI chains was investigated in addition to cover this temperature area.

An MMFF conformer distribution on a single LPEI dimer yielded seven lowest strain energy conformers within 3.3 kJ/mol of each other and accounting for 80% in the cumulative Boltzmann weights. Four of these conformers show β-amine−amine interactions. The best conformer, representing 23.9% in the Boltzmann weights, shows even two β-amine−amine interactions with NH−NH−N distances of 2.526 and 2.514 Å. Such a geometry is suited to capture CO_2 with a β-amine as the internal catalyst. Figure 7 shows the CO_2 capturing process with a single chain of LPEI. The CO_2-physisorption complex (a) has a ΔH of −13.3 kJ/mol. The animation of the imaginary vibration of the transition state (b) is very similar to the one described in Figure 5. The forward and backward activation barriers are 98.2 and 87.0 kJ/mol, respectively, considerably higher as in the case of a pair of LPEI chains. This is due to sterical strain. The carbamic acid in its anti-configuration (c) still resembles the geometry of the transition state (b) and shows a H-bridge of the (CO)OH to the amine, while in the final product, the carbamic acid (d) H-bridges between the remaining amines and between an amine and the O═C(OH)

https://doi.org/10.1021/acs.iecr.1c00846
Ind. Eng. Chem. Res. 2021, 60, 11309−11316

are present. In the absence of a second LPEI chain, the overall reaction enthalpy is −12.9 kJ/mol only. However, there is no reason to assume that H-bridging with a secondary amine of another chain would not be possible with a similar reaction enthalpy as found for the pair of LPEI chains, but with a substantial lower proximity, resulting in an average value lower than −54.2 kJ/mol. Very similar values were obtained for the other conformers with β-amine−amine interactions, so the higher activation barriers are partly compensated by a higher availability.

Geometry optimizations applying the C-PCM model with an ε = 7.43, the nonpolar solvent situation, yielded three structures with an energy difference of only 0.5 kJ/mol: the amine carbamic acid in its anti-conformation, the amine carbamic acid, and the ammonium carbamate. However, as already stated above, H-bridging of the carbamic acid with a secondary amine of another chain would lead to a far more stable amine carbamic acid complex, very similar to the outcome of the calculations discussed for the pair of LPEI chains.

The computational results on CO_2 capture under dry conditions clearly indicate the following:

1. The crystalline part of LPEI, the double-stranded helix structure, does not contribute to the CO_2 capturing process due to the complete shielding of the secondary amines.
2. Pairs of LPEI chains, present in amorphous regions of LPEI below its melting point until ∼5 °C above, have multiple sites consisting of two secondary amines on each chain, allowing fast and reversible carbamic acid formation with an adsorption enthalpy in line with experimental observations.
3. At temperatures >5 °C above the melting point of LPEI, fast reversible carbamic acid formation by single chains of LPEI is possible, catalyzed by a secondary amine in the β-position.
4. A more in-depth analysis of the nature of amine carbamic acid complexes applying either B3LYP or MO6-2X functionals with various basis sets and B3LYP calculations using the C-PCM solvation model yielded that the predominant form should be the amine carbamic acid complex with only a very minor amount of the ammonium carbamate complex.

Humid Conditions. Under humid conditions, the CO_2 uptake of LPEI impregnated on hydrophilic and hydrophobic silicas was enhanced at temperatures from 25 to 55 °C.[31] The highest enhancement was observed at 25 °C at specific humidities of 11.5 and 15.3 mg H_2O/g sorbent and 44.5% loading of LPEI on fumed silica. These humidity values correspond to a H_2O uptake of 6.4 and 10.5 mmol H_2O/g at 25 °C, respectively. The CO_2 uptake at 25 °C under these conditions was 4.1 mmol/g adsorbent. As discussed earlier, the addition of H_2O to crystalline LPEI leads to the formation of an LPEI/0.5 H_2O phase. A H_2O uptake of 10.5 mmol/g is close to LPEI/0.5 H_2O.

An LPEI−dimer pair 3 H_2O complex was chosen as a model to investigate the formation of carbamic and carbonic acid by secondary amines. Table 1 lists ΔH-CO_2 and activation barriers of the two options.

The ΔH-CO_2 of the complex leading to carbamic acid is lower than the ΔH-CO_2 of the complex leading to carbonic acid and both of them are significantly lower than ΔH-CO_2 of the LPEI dimer pair leading to carbamic acid under dry conditions. However the activation enthalpy for carbonic acid formation is much lower than the activation enthalpy for carbamic acid formation, thus largely favoring carbonic acid formation. Figure 8 shows the CO_2-physisorption complex (a), the transition state (b), and the H_2CO_3 anti-complex (c).

Table 1. ΔH' Values of CO_2 Complexes and Activation Enthalpies (E_a) of the LPEI Dimer Pair 3 H_2O CO_2 Complexes as Models for CO_2 Capture

complex	product	ΔH CO_2 (kJ/mol)	E_a (kJ/mol)
LPEI dimer pair 3 H_2O−CO_2 complex	carbamic acid	−28.0	66.4
	carbonic acid	−24.7	42.7

From Figure 4 in space filling display, it can be seen that the all-trans structure of the LPEI/0.5 H_2O chains leads to void spaces between alternating amine groups. These spaces are large enough for CO_2 and H_2O to diffuse inside by normal internal thermal movement of the structure. The $LPEI_2$ 3 H_2O CO_2 complex (a) has a H_2O−CO_2 distance of 2.591 Å. The transition state $LPEI_2$ 3 H_2O CO_2 (b) has a H_2O−CO_2 distance of 1.598 Å. The animation of the imaginary vibration of the transition state shows simultaneous formation of the O−CO_2 bond, proton transfer from H_2O to the secondary amine in the front, and proton transfer from the secondary amine in the front to O(CO_2). The secondary amine in the back maintains its H-bridge to H_2O as in the initial CO_2 complex. The H_2CO_3 anti-complex (c) has H-bridges to both secondary amines, and its structure still resembles the transition state. It is generally known that H_2CO_3 itself has very limited stability. However, in this case, H_2CO_3 in its anti-form is stabilized by two H-bridges of the two LPEI chains. H_2CO_3 in its best form can also be stabilized by two H-bridges of the two LPEI chains, however at the cost of a slightly increased distance between the two LPEI chains. That stabilization is 22.6 kJ/mol less than the stabilization of H_2CO_3 in its anti-form. The corresponding ammonium bicarbonates are not stable species according to B3LYP/6-31G*. Applying the C-PCM model for a nonpolar solvent (ε = 7.43), the corresponding ammonium bicarbonates are stable. Again the ammonium bicarbonate anti-species is by far the most stable one of the two and 1.4 kJ/mol more stable than the secondary amine−carbonic acid complex. Thus, it seems very likely that CO_2 is captured as an $R_2NH_2^+$ HCO_3^- and a H_2CO_3 anti-complex in a ratio of approximately 2/1.

The computational results on CO_2 capture under humid conditions clearly indicate that:

1. Crystalline LPEI under humid conditions is transformed into an LPEI/0.5 H_2O type of phase.
2. The LPEI/0.5 H_2O type of phase, apart from being more open to additional H_2O and CO_2 molecules, has a very suitable geometry for capturing CO_2 yielding exclusively $R_2NH_2^+$ HCO_3^- and R2NH H_2CO_3 complexes in a ratio of 2/1. Both the strong CO_2 physisorption complex and its low-lying transition state contribute to that process.
3. The formation of carbamic acid from an LPEI/0.5 H_2O type of phase can be excluded as its activation barrier is significantly higher than the activation barrier for H_2CO_3 formation.

https://doi.org/10.1021/acs.iecr.1c00846
Ind. Eng. Chem. Res. 2021, 60, 11309−11316

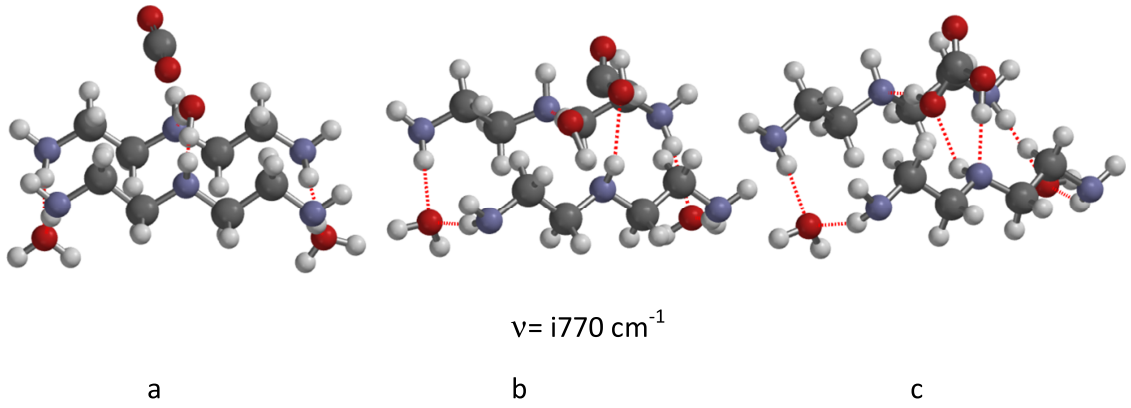

Figure 8. $LPEI_2$ 3 H_2O complex as a model for CO_2 uptake: (a) ($LPEI_2$ 3 H_2O CO_2), (b) transition state ($LPEI_2$ 3 H_2O CO_2), and (c) ($LPEI_2$ 2 H_2O)($NHCO_2H$-anti). B3LYP/6-31G*; display model: ball & spoke with C: gray, N: blue, and H: white. H-bridges: red dotted lines.

All transition states discussed are of the type described by Said et al.,[14] characterized by a six-membered ring with simultaneous formation of the N−C(CO_2) or O−C(CO_2) bond, proton transfer from the first amine to the second amine, and proton transfer from the second amine to O(CO_2). They also do follow the general trends and influences, as described by Lee and Kitchin.[13] Despite the agreement with these general trends, it is still crucial to start analyzing the experimental structural data, and from there developing geometrical models to obtain reliable data on physisorption, activation, and reaction enthalpies. Only in this way, the sharp discrimination between the CO_2 capturing reactions under dry and humid process conditions was found: dry conditions lead to carbamic acid formation and humid conditions lead to ammonium bicarbonate/ amine carbonic acid formation.

Strictly taken, the conclusions of this study are valid for LPEI only. From the obvious similarities between LPEI and branched (B)PEI in the experimental studies[30,31] it is tempting to suggest analogous reaction mechanisms but this has to be studied separately as also differences are observed.

Finally, LPEI seems suited to capture CO_2 from large point emission sources like power or steel making plants, as only in such an environment CO_2 capture can be carried out with a rather constant H_2O level during CO_2 sorption and desorption to maintain the enhanced CO_2 uptake capacity of an LPEI/0.5 H_2O type of phase while at the same time avoiding huge energy consumption due to the condensation and evaporation of large amounts of H_2O. With respect to the latter, the material seems not to be suited for direct air capture of CO_2 where the amount of water varies largely as a function of fluctuating weather conditions due to day/night rhythm and seasons and the CO_2/H_2O ratio is several magnitudes lower.

■ ASSOCIATED CONTENT

Supporting Information

The Supporting Information is available free of charge at https://pubs.acs.org/doi/10.1021/acs.iecr.1c00846.

Molecular structures pdb, guide to molecular structures pdb (ZIP)

■ AUTHOR INFORMATION

Corresponding Author

W. Buijs − *Engineering Thermodynamics, Process & Energy Department, Faculty of Mechanical, Maritime and Materials Engineering, Delft University of Technology, 2628 CB Delft, The Netherlands;* orcid.org/0000-0003-3273-5063; Email: w.buijs@tudelft.nl

Complete contact information is available at: https://pubs.acs.org/10.1021/acs.iecr.1c00846

Notes

The author declares no competing financial interest.

■ ACKNOWLEDGMENTS

The author wants to thank Guillaume Herlem for kindly providing the crystal structure of anhydrous PEI.

■ REFERENCES

(1) IPCC. Summary for Policymakers. In *Climate Change 2013*; The Physical Science Basis. Contribution of Working Group I to the Fifth Assessment Report of the Intergovernmental Panel on Climate Change; Stocker, T. F.; Qin, D.; Plattner, G.-K.; Tignor, M.; Allen, S. K.; Boschung, J.; Nauels, A.; Xia, Y.; Bex, V.; Midgley, P. M., Eds.; Cambridge University Press: Cambridge, United Kingdom and New York, NY, USA, 2013.

(2) EPA United States Environmental Protection Agency. U.S. Carbon Dioxide Emissions, 2020. https://www.epa.gov/ghgemissions/overview-greenhouse-gases.

(3) Choi, S.; Drese, J. H.; Jones, C. W. Adsorbent Materials for Carbon Dioxide Capture from Large Anthropogenic Point Sources. *ChemSusChem* **2009**, *2*, 796−854.

(4) Goeppert, A.; Zhang, H.; Czaun, M.; May, R. B.; Prakash, G. K. S.; Olah, G. A.; Narayanan, R. R. Easily Regenerable Solid Adsorbents Based on Polyamines for Carbon Dioxide Capture from the Air. *ChemSusChem* **2014**, *7*, 1386−1397.

(5) Sanz-Pérez, E. S.; Murdock, C. R.; Didas, S. A.; Jones, C. W. Direct Capture of CO2 from Ambient Air. *Chem. Rev.* **2016**, *116*, 11840−11876.

(6) Shen, X.; Du, H.; Mullins, R. H.; Kommalapati, R. R. Polyethylenimine Applications in Carbon Dioxide Capture and Separation: From Theoretical Study to Experimental Work. *Energy Technol.* **2017**, *5*, 822−833.

(7) Veneman, R.; Zhao, W.; Li, Z.; Cai, N.; Brilman, D. W. F. Adsorption of CO2 and H2O on supported amine sorbents. *Energy Procedia* **2014**, *63*, 2336−2345.

(8) Alesi, W. R., Jr; Kitchin, J. R. Evaluation of a primary amine functionalized ion-exchange resin for CO2 capture. *Ind. Eng. Chem. Res.* **2012**, *51*, 6907−6915.

(9) Min, K.; Choi, W.; Kim, C.; Choi, M. Oxidation-stable amine containing adsorbents for carbon dioxide capture. *Nat. Commun.* **2018**, *9*, No. 726.

(10) Buijs, W. Direct Air Capture of CO2 with an Amine Resin: A Molecular Modeling Study of the Oxidative Deactivation Mechanism with O_2. *Ind. Eng. Chem. Res.* **2019**, *58*, 17760−17767.
(11) Buijs, W. Direct Air Capture of CO2 with an Amine Resin: A Molecular Modeling Study of the Deactivation Mechanism by CO2. *Ind. Eng. Chem. Res.* **2019**, *58*, 14705−14708.
(12) Buijs, W. Molecular Modeling Study of the SO2 Deactivation of an Amine Resin and a Procedure To Avoid SO2 Deactivation Using a Polyethylene Glycol/Tertiary Amine System. *Ind. Eng. Chem. Res.* **2020**, *59*, 13388−13395.
(13) Lee, A. S.; Kitchin, J. R. Chemical and Molecular Descriptors for the Reactivity of Amines with CO2. *Ind. Eng. Chem. Res.* **2012**, *51*, 13609−13618.
(14) Said, R. B.; Kolle, J. M.; Essalah, K.; Tangour, B.; Sayari, A. A Unified Approach to CO2-Amine Reaction Mechanisms. *ACS Omega* **2020**, *5*, 26125−26133.
(15) Buijs, W.; de Flart, S. Direct Air Capture of CO2 with an Amine Resin: A Molecular Modeling Study of the CO2 Capturing Process. *Ind. Eng. Chem. Res.* **2017**, *56*, 12297−12304.
(16) Spartan '18 is a product of Wavefunction Inc., 18401 Von Karman Avenue, Suite 370, Irvine, CA 92612, U.S.A, 2021. www.wavefun.com.
(17) Kazazi, M.; Afshar, A.; Sajjadnejad, M. The Inhibition Effect of Polyethylenimine (PEI) on Pitting Corrosion of 304 Austenitic Stainless Steel in 3.5% NaCl Solution. *Int. J. ISSI* **2013**, *10*, 14−22.
(18) Finšgar, M.; Fassbender, S.; Nicolini, F.; Milošev, I. Polyethyleneimine as a corrosion inhibitor for ASTM 420 stainless steel in near-neutral saline media. *Corros. Sci.* **2009**, *51*, 525−533.
(19) Shahzad, K.; Sliem, M. H.; Shakoor, R. A.; Radwan, A. B.; Kahraman, R.; Umer, M. A.; Manzoor, U.; Abdullah, A. M. Electrochemical and thermodynamic study on the corrosion performance of API X120 steel in 3.5% NaCl solution. *Sci. Rep.* **2020**, *10*, No. 4314.
(20) Boussif, O.; Lezoualc'h, F.; Zenta, M. A.; Mergny, M. D.; Scherman, D.; Demeneix, B.; Behr, J.-P. A versatile vector for gene and oligonucleotide transfer into cells in culture and in vivo: Polyethylenimine. *Proc. Natl. Acad. Sci. U.S.A.* **1995**, *92*, 7297−7306.
(21) Herlem, G.; Lakard, B.; Fahys, B. *Recent Research Developments in Electroanalytical Chemistry*; Transworld Research Network: Trivandrum, India, 2001; Vol. 3, pp 21−33. ISBN 81-7895-010-3.
(22) Andersson, M. M.; Hatti-Kaul, R. Protein stabilising effect of polyethyleneimine. *J. Biotechnol.* **1999**, *72*, 21−31.
(23) Torres, R.; Mateo, C.; Fuentes, M.; Palomo, J. M.; Ortiz, C.; Fernández- Lafuente, R.; Guisan, J. M. Reversible Immobilization of Invertase on Sepabeads Coated with Polyethyleneimine: Optimization of the Biocatalyst's Stability. *Biotechnol. Prog.* **2002**, *18*, 1221−1226.
(24) Chatani, Y.; Tadokoro, H.; Saegusa, T.; Ikeda, H. Structural Studies of Poly(ethylenimine). 1. Structures of Two Hydrates of Poly(ethylenimine): Sesquihydrate and Dihydrate. *Macromolecules* **1981**, *14*, 315−321.
(25) Chatani, Y.; Kobatake, T.; Tadokoro, H.; Tanaka, R. Structural Studies of Poly(ethylenimine). 2. Double-Stranded Helical Chains in the Anhydrate. *Macromolecules* **1982**, *15*, 170−176.
(26) Chatani, Y.; Kobatake, T.; Tadokoro, H. Structural Studies of Poly(ethylenimine). 3. Structural Characterization of Anhydrous and Hydrous States and Crystal Structure of the Hemihydrate. *Macromolecules* **1983**, *16*, 199−204.
(27) Hashida, T.; Tashiro, K.; Aoshima, S.; Inaki, Y. Structural Investigation on Water-Induced Phase Transitions of Poly(ethylene imine). 1. Time-Resolved Infrared Spectral Measurements in the Hydration Process. *Macromolecules* **2002**, *35*, 4330−4336.
(28) Hashida, T.; Tashiro, K.; Inaki, Y. Structural Investigation of Water-Induced Phase Transitions of Poly(ethylene imine). III. The Thermal Behavior of Hydrates and the Construction of a Phase Diagram. *J. Polym. Sci., Part B: Polym. Phys.* **2003**, *41*, 2937−2948.
(29) Hashida, T.; Tashiro, K. Structural Study on Water-induced Phase Transitions of Poly(ethylene imine) as Viewed from the Simultaneous Measurements of Wide-Angle X-ray Diffractions and DSC Thermograms. *Macromol. Symp.* **2006**, *242*, 262−267.
(30) Zhang, H.; Goeppert, A.; Prakash, G. K. S.; Olah, G. Applicability of linear polyethylenimine supported on nano-silica for the adsorption of CO2 from various sources including dry air. *RSC Adv.* **2015**, *5*, 52550−52562.
(31) Zhang, H.; Goeppert, A.; Olah, G.; Prakash, G. K. S. Remarkable effect of moisture on the CO2 adsorption of nano-silica supported linear and branched polyethylenimine. *J. CO2 Util.* **2017**, *19*, 91−99.
(32) Cambridge Structural Database. https://www.ccdc.cam.ac.uk/ (accessed Jan 31, 2021).
(33) Herlem, G.; Lakard, B. Ab initio study of the electronic and structural properties of the crystalline polyethyleneimine polymer. *J. Chem. Phys.* **2004**, *120*, 9376−9382.
(34) A List of Thermodynamical Properties of Water. https://www.engineeringtoolbox.com/water-thermal-properties-d_162.html (accessed Jan 31, 2021).
(35) Tomasi, J.; Mennucci, B.; Cammi, R. Quantum mechanical continuum solvation models. *Chem. Rev.* **2005**, *105*, 2999−3093.
(36) Didas, S. A.; Sakwa-Novak, M. A.; Foo, G. S.; Sievers, C.; Jones, C. W. Effect of amine surface coverage on the Co-adsorption of CO2 and water: spectral deconvolution of adsorbed species. *J. Phys. Chem. Lett.* **2014**, *5*, 4194−4200.
(37) Hahn, M. W.; Andreas Jentys, M. S.; Lercher, J. A. Mechanism and kinetics of CO2 adsorption on surface bonded amines. *J. Phys. Chem. C* **2015**, *119*, 4126−4135.
(38) Yu, J.; Chuang, S. S. C. The structure of adsorbed species on immobilized amines in CO2 capture: an in situ IR study. *Energy Fuels* **2016**, *30*, 7579−7587.
(39) Mafra, L.; Cendak, T.; Schneider, S.; Wiper, P. V.; Pires, J.; Gomes, J. R. B.; Pinto, M. L. Structure of chemisorbed CO2 species in amine-functionalized mesoporous silicas studied by solid-state NMR and computer modelling. *J. Am. Chem. Soc.* **2017**, *139*, 389−408.
(40) Afonso, R.; Sardo, M.; Mafra, L.; Gomes, J. R. B. Unravelling the Structure of Chemisorbed CO2 Species in Mesoporous Aminosilicas: A Critical Survey. *Environ. Sci. Technol.* **2019**, *53*, 2758−2767.
(41) Dielectric Constant for PEI. https://omnexus.specialchem.com/polymer-properties/properties/dielectric-constant (accessed June 26, 2021).

https://doi.org/10.1021/acs.iecr.1c00846
Ind. Eng. Chem. Res. 2021, 60, 11309−11316